

Improved Hamiltonians for Quantum Simulations

Marcela Carena,^{1,2,3,4,*} Henry Lamm,^{1,†} Ying-Ying Li,^{1,‡} and Wanqiang Liu^{4,§}

¹*Fermi National Accelerator Laboratory, Batavia, Illinois, 60510, USA*

²*Enrico Fermi Institute, University of Chicago, Chicago, Illinois, 60637, USA*

³*Kavli Institute for Cosmological Physics, University of Chicago, Chicago, Illinois, 60637, USA*

⁴*Department of Physics, University of Chicago, Chicago, Illinois, 60637, USA*

(Dated: March 8, 2022)

The quantum simulation of lattice gauge theories for the foreseeable future will be hampered by limited resources. The historical success of Symanzik-improved lattice actions in classical simulations strongly suggests that improved Hamiltonians will reduce quantum resources for fixed discretization errors. In this work, we consider Symanzik-improved lattice Hamiltonians for pure gauge theories and design quantum circuits for $\mathcal{O}(a^2)$ -improved Hamiltonians in terms of primitive group gates. An explicit demonstration for \mathbb{Z}_2 is presented including exploratory tests using the `ibm_perth` device.

Quantum simulations of lattice field theories avoid the exponentially large resources which plague classical methods for finite-density and dynamics [1–3]. While such resource reduction is dramatic for problems of interest like transport coefficients [4], PDFs [5–7], and the strong-CP problem [8, 9], the number of qubits remains $\mathcal{O}((L/a)^d)$ for a d spatial dimensional lattice of physical length L and spacing a . An important question for such simulations is what resources are required for practical quantum advantage. Here, we will consider QCD as our fiducial case. Current estimates suggest ~ 10 qubits per gluon link are required [10–16]. This implies that kilobyte-sized computers are required for 3+1d $SU(3)$ simulations with smaller requirements for $U(1)$ and $SU(2)$ [10–14, 17–34]. Comparable resources are found for qudit devices [14, 35, 36].

To estimate gate costs, one must specify a Hamiltonian for the simulations. Most studies of gauge theories consider the Kogut-Susskind Hamiltonian, \hat{H}_{KS} [37]:

$$\hat{H}_{KS} = \hat{K}_{KS} + \hat{V}_{KS}, \quad (1)$$

$$\hat{K}_{KS} = \sum_{x,i} \frac{g_i^2}{a} \text{Tr} \hat{L}_i^2(x), \quad \hat{V}_{KS} = - \sum_{x,i < j} \frac{2}{g_s^2 a} \text{Re Tr} \hat{P}_{ij}(x).$$

which has discretization errors of $\mathcal{O}(a^2)$. The electric field $\hat{L}_i(x)$ is the left generator of gauge transformations on a link $U_i(x)$ [38] while $\hat{P}_{ij}(x)$ is the spatial plaquette term (e.g. $U_1 U_7 U_5^\dagger U_6^\dagger$ in Fig. 1).

When approximating the time evolution operator $\mathcal{U}(t) = e^{-i\hat{H}_{KS}t}$ via trotterization, the gate count scales $\propto t^{3/2}(L/a)^{3d/2}\epsilon^{-1/2}$ [39, 40] for a maximum error ϵ for any state; although logarithmic corrections may prove important [15]. For one candidate for early practical quantum advantage in $SU(3)$ – the shear viscosity η , a loose

upper bound of $\mathcal{O}(10^{49})$ T gates has been estimated [15] where the authors assumed $\epsilon = 10^{-8}$. Given that lattice errors of $\mathcal{O}(a^2, e^{-L/a})$ are not accounted for in ϵ and that current theoretical uncertainties on η are $\mathcal{O}(1)$ [41], $\epsilon \sim 10^{-2}$ seems a better target for practical quantum advantage. A tighter bound could be obtained by requiring that only low-lying states have errors below ϵ . This greatly reduces the L dependence and prefactors in the gate costs [42, 43]. Even with these reductions the gate cost is expected to be beyond access on near-term devices.

Further exacerbating these problems is the current, noisy status of quantum computers and the open question of how much quantum error correction is required to perform such simulations. General estimates suggest $\mathcal{O}(10^{1-5})$ physical qubits per logical qubit [44–46] – so physical qubit requirements could easily rise to the megabyte scale.

Gate reductions may be possible using other approximations of $\mathcal{U}(t)$ [47–52]. At the cost of classical signal-to-noise problems, stochastic state preparation yields shallower circuits [53–56]. Furthermore, performing scale setting classically can reduce quantum resources [57–59]. Lattice field theory specific error correction or mitigation could also potentially decrease quantum costs [60, 61].

In this *letter*, we present a new direction for reducing quantum resources by using Symanzik-improved Hamiltonians. The Symanzik program [62–64] has taught us that dramatic reductions in computational resources are possible through the use of lattice theories with reduced discretization errors. To do this, one includes specific additional terms in the Hamiltonian, and uses their relative weight to cancel the leading discretization errors [65, 66]. For example, \hat{V}_{KS} can be series expanded via \hat{P}_{ij} ,

$$\hat{P}_{ij} = \mathbb{1} - \frac{g_s^2 a^4}{2} \left[F_{ij}^2 + \frac{a^2}{12} F_{ij} (D_i^2 + D_j^2) F_{ij} + \mathcal{O}(a^4) \right]. \quad (2)$$

The deviations between lattice and continuous quantum field theories arise not only from discretizing the classical Hamiltonian, but also at the quantum level in the path integral. By adding rectangular and bent six-link loop terms (Fig. 1) to \hat{H}_{KS} , the $F_{ij}(D_i^2 + D_j^2)F_{ij}$ term can

* carena@fnal.gov

† hlyamm@fnal.gov

‡ Corresponding author: yingying@fnal.gov

§ wanqiangl@uchicago.edu

be canceled resulting in a leading order $\mathcal{O}(a^4)$ errors. Including only the rectangular term, one can remove the classical $\mathcal{O}(a^2)$ error, leaving the quantum $\mathcal{O}(g_s^2 a^2)$ error.

We will define our improved Hamiltonian as $\hat{H}_I = \hat{K}_I + \hat{V}_I$ with improved potential term $\hat{V}_I = \beta_{V0}\hat{V}_{KS} + \beta_{V1}\hat{V}_{\text{rect}} + \beta_{V2}\hat{V}_{\text{bent}}$. \hat{V}_{rect} is defined as

$$\hat{V}_{\text{rect}} = \frac{2}{ag_s^2} \sum_{x,i < j} \text{Re Tr} \left[\hat{R}_{ij}(x) + \hat{R}_{ji}(x) \right], \quad (3)$$

where $\hat{R}_{ij}(x)$ (e.g. $U_1 U_2 U_3 U_4^\dagger U_5^\dagger U_6^\dagger$ in Fig. 1) is the 6-link rectangular loop term with the i -th (j -th) direction crossing two units (one unit) of lattice spacing. \hat{V}_{bent} has analogous expressions to \hat{V}_{rect} . The couplings are constrained by $\beta_{V0} + 8\beta_{V1} + 16\beta_{V2} = 1$ for a consistent definition of g_s [63]. For classical improvement, the couplings are $\beta_{V0} = \frac{5}{3}$, $\beta_{V1} = -\frac{1}{12}$, $\beta_{V2} = 0$. While classically $\beta_{V2} = 0$, it is generated at $\mathcal{O}(g^2 a^2)$ [64] but remains suppressed relative to β_{V1} [67]. To obtain an improved kinetic term $\hat{K}_I = \beta_{K0}\hat{K}_{KS} + \beta_{K1}\hat{K}_{2L}$, one includes the two-link term:

$$\hat{K}_{2L} = \frac{g_t^2}{a} \sum_{x,i} \text{Tr} \left[\hat{L}_i(x) \hat{U}_i(x) \hat{L}_i(x + a\vec{i}) \hat{U}_i^\dagger(x) \right]. \quad (4)$$

$\beta_{K0,1}$ are constrained by $\beta_{K0} + \beta_{K1} = 1$ [66] for a consistent definition of g_t . Classical errors of $\mathcal{O}(a^2)$ are cancelled when $\beta_{K0} = \frac{5}{6}$ and $\beta_{K1} = \frac{1}{6}$ [66]. Similar to \hat{H}_{KS} , the improved Hamiltonian can also be obtained from an improved action via the transfer matrix [65].

For the Lüscher-Weisz action [63], $a = 0.4$ fm lattices were found to have similar discretization errors to $a = 0.17$ fm lattices with the Wilson action [68]. Given that \hat{H}_I is derivable from the Lüscher-Weisz action [65, 66], it is unsurprising that similar scaling is suggested by the limited studies in the Hamiltonian formalism [69]. Therefore, using \hat{H}_I may require $\gtrsim 2^d$ fewer qubits in realistic quantum simulations for a fixed discretization error compared to \hat{H}_{KS} .

So far, we have only discussed the classically-improved couplings. For determining the quantum-corrected couplings, a number of methods exist. Perturbative calculations of the couplings in the Hamiltonian formalism analogous to those in [63] could be obtained. To remove these $\mathcal{O}(g^2 a^2)$ errors, one should nonperturbatively tune the couplings via lattice computations. Part of the tuning can be done by resumming tadpole contributions [67, 70, 71]. As non-perturbatively determining the couplings on quantum computers will cost considerable resources, one may opt to extract them via the analytic continuation of classical computations [59].

While we occupy ourselves with the improvements to the gauge Hamiltonian, the $\mathcal{O}(a)$ fermionic Hamiltonian should be improved as well. Many methods exist in the action formulations. Some preliminary work in formulating $1+1d$ improved fermions has been considered [72] but

more work is required – particularly for the interesting case of chiral fermions.

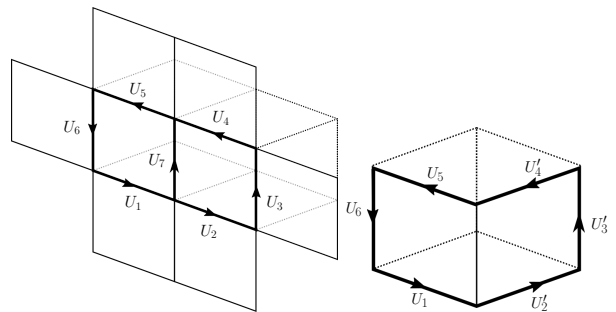


FIG. 1: 3d lattices with links labeled as used in the text for the plaquette, rectangle, and the bent loop term.

We construct quantum circuits to implement the improvement terms in Eq. (3) and Eq. (4) for a generic gauge theory, using the primitive gates acting on group element registers [73]: the inverse gate \mathfrak{U}_{-1} , the left/right product gates $\mathfrak{U}_x^{L/R}$, the trace gate \mathfrak{U}_{Tr} , the Fourier transform gate \mathfrak{U}_F and a phase gate $\mathfrak{U}_{\text{phase}}$. The improved potential term includes the square Wilson loops $\hat{P}_{ij}(x)$ for every individual plaquette and the rectangle ones $\hat{R}_{ij}(x)$ for every neighboring two plaquettes in the spatial lattice. The group element basis $|U\rangle$ diagonalizes both \hat{P}_{ij} and \hat{R}_{ij} . Optimal quantum circuits depend on the underlying architecture – in particular connectivity. We present the quantum circuits that only require register connectivity between every pair of links sharing one common site (linear register connectivity). The circuit for the rectangle one $\mathcal{U}_{V_{\text{rect}}} = e^{-i\theta \text{Re Tr} \hat{R}_{ij}(x)}$ is shown in Fig. 2, with the coupling and trotter step information encoded in the parameter θ . The same circuit as Fig. 2 with registers U_2, U_3, U_4 replaced by U'_2, U'_3, U'_4 in Fig. 1 implements $\mathcal{U}_{V_{\text{bent}}}$. The circuit for the unimproved potential term can be constructed similarly to that in Ref. [73] but with linear register connectivity.

The unimproved kinetic term can be implemented by $\mathfrak{U}_{\text{phase}}$ in the Fourier basis which diagonalizes $\hat{L}_i^2(x)$ [73]. To construct a circuit for the two-link term \hat{K}_{2L} in Eq. (4) and avoid dealing with \hat{L} and \hat{U} operators simultaneously,

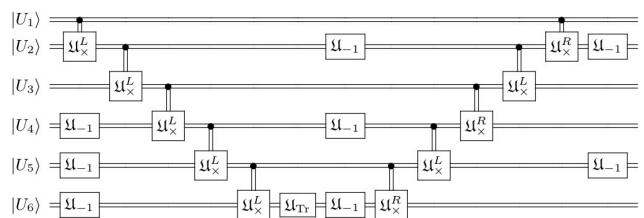


FIG. 2: $\mathcal{U}_{V_{\text{rect}}}$ assuming linear register connectivity.

we will rewrite it using the right electric field operator [38]:

$$\begin{aligned}\hat{R}_i(x) &\equiv \hat{U}_i^\dagger(x)\hat{L}_i(x)\hat{U}_i(x) = \hat{R}_i^b(x)T_b, \\ \hat{R}_i^b(x) &= 2 \text{Tr}[\hat{U}_i^\dagger(x)\hat{L}_i(x)\hat{U}_i(x)T_b].\end{aligned}\quad (5)$$

With $\hat{R}_i(x)$, we can then construct \hat{K}_{2L} term by term as

$$\hat{K}_{2L} = \frac{g_t^2}{a} \sum_{x,i} \text{Tr}[\hat{R}_i(x)\hat{L}_i(x + a\vec{i})], \quad (6)$$

where summands commute.

For simplicity, we denote the two succeeding links in one direction as U_1 and U_2 following Fig. 1. For Abelian gauge theories, $\hat{R}_i(x) = \hat{L}_i(x)$, $\hat{R}_1\hat{L}_2$ can be straightforwardly implemented in the Fourier basis. There are at least two obstacles in non-Abelian gauge theories. Firstly, $\hat{R}_1^c\hat{L}_2^c$ with different c do not commute, and Hamiltonians as sums of non-commuting terms are in general difficult to implement. Secondly, for a generic discrete non-Abelian group, although \hat{L}^2 is easy to define through the group Fourier transformation, for \hat{L}^c it is less clear. We can bypass both obstacles by decomposing $\hat{R}_1\hat{L}_2$ as

$$\text{Tr}(\hat{R}_1\hat{L}_2) = \frac{1}{2} \text{Tr}[\hat{L}_2^2 + \hat{R}_1^2 - (\hat{L}_2 - \hat{R}_1)^2]. \quad (7)$$

With $\hat{R}^2 = \hat{L}^2$, the first two terms can be absorbed into \hat{K}_{KS} by taking β_{K0} to $\beta_{K0} + \beta_{K1} = 1$. Thus, for \hat{K}_I the only new term is $\text{Tr}(\hat{L}_2 - \hat{R}_1)^2$, which commutes with $\hat{U}_1\hat{U}_2$. Defining the evolution operator $\mathcal{U}_{K_{2L}} \equiv e^{i\theta \text{Tr}(\hat{L}_2 - \hat{R}_1)^2}$, the matrix elements $\langle U'_1, U'_2 | \mathcal{U}_{K_{2L}} | U_1, U_2 \rangle$ are only non-zero for $U'_1 U'_2 = U_1 U_2$. We can write down the following expression:

$$\langle U'_1, U'_2 | \mathcal{U}_{K_{2L}} | U_1, U_2 \rangle = \delta(U'_1 U'_2 - U_1 U_2) \mathcal{A}(U_1, U_2, U'_1). \quad (8)$$

By integrating over U'_2 and changing the variable U'_2 to $V \equiv U'_2 U_2^{-1} = e^{i\alpha_c T^c}$, we can determine $\mathcal{A}(U_1, U_2, U'_1)$. Using the invariance of the Haar measure and the property $\langle U'_1, V U_2 | = \langle U'_1, U_2 | e^{i\alpha_c \hat{L}_2^c}$, we have:

$$\mathcal{A}(U_1, U_2, U'_1) = \langle U'_1, U_2 | \int dV e^{i\alpha_c \hat{L}_2^c} \mathcal{U}_{K_{2L}} | U_1, U_2 \rangle. \quad (9)$$

The integral over all group transformations $\int dV e^{i\alpha_c \hat{L}_2^c}$ is equivalent to projecting the U_2 register to the ground state of \hat{L}_2^2 ($|J_2 = 0\rangle$) up to a normalization factor fixed to be consistent with $\int dV = |G|$ [74]:

$$\int dV e^{i\alpha_c \hat{L}_2^c} = |G| |J_2 = 0\rangle \langle J_2 = 0| = |G| \hat{P}_{J_2=0}. \quad (10)$$

Substitute Eq. (10) into Eq. (9) and notice that, as $\mathcal{U}_{K_{2L}}$ commutes with \hat{R}_2^2 , it conserves the quantum number J_2 , and therefore, $\hat{P}_{J_2=0} \mathcal{U}_{K_{2L}} = \hat{P}_{J_2=0} \mathcal{U}_{K_{2L}} \hat{P}_{J_2=0}$. Insert another $\hat{P}_{J_2=0}$ after $\mathcal{U}_{K_{2L}}$ in Eq. (9) and we find \mathcal{A} is:

$$\begin{aligned}\mathcal{A}(U_1, U_2, U'_1) &= \langle U'_1, J_2 = 0 | \mathcal{U}_{K_{2L}} | U_1, J_2 = 0 \rangle \\ &= \langle U'_1 | e^{i\theta \text{Tr} \hat{R}_1^2} | U_1 \rangle.\end{aligned}\quad (11)$$

Using Eq. (11), the circuit in Fig. 3 implements Eq. (8) by first storing the conserved quantity $U_1 U_2$ in the $|U_2\rangle$ register via \mathcal{U}_\times^L , and then performing $e^{i\theta \hat{R}_1^2}$ on $|U_1\rangle$ with the sequence $\mathcal{U}_F^\dagger \mathcal{U}_{\text{phase}} \mathcal{U}_F$ gates. Finally, we multiply back to ensure the conserved product using the information stored in $|U_2\rangle$ via $\mathcal{U}_{-1} \mathcal{U}_\times \mathcal{U}_{-1}$.

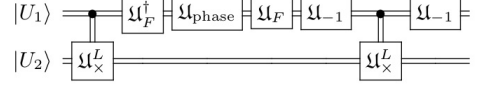


FIG. 3: Quantum circuit for $\mathcal{U}_{K_{2L}}$.

Gate	$\hat{K}_{KS} + \hat{V}_{KS}$	$\hat{K}_{2L} + \hat{V}_{\text{rect}}$
\mathcal{U}_F	2	2
$\mathcal{U}_{\text{phase}}$	1	1
\mathcal{U}_{Tr}	$\frac{d-1}{2}$	$d-1$
\mathcal{U}_{-1}	$3(d-1)$	$2 + 8(d-1)$
\mathcal{U}_\times	$6(d-1)$	$4 + 20(d-1)$

TABLE I: Number of primitive gates per link register in d spatial dimensions, for a single trotter step neglecting boundary effects.

While using \hat{H}_I should require $\gtrsim 2^d$ times fewer qubits, it requires more gates per link register. Since the dominant quantum errors today are the $\mathcal{O}(10^{-2})$ two-qubit gate error rates and decoherence [75–77], this increased cost may lead to consternation. We list the gate costs for a general gauge group in terms of primitive gates in Tab. I for one trotter step using both \hat{H}_{KS} and \hat{H}_I . Studies of \mathbb{Z}_N and D_N [78] suggest that different primitive gates take approximately the same order of entangling native gates. Depending on which primitive gates dominate the circuits, the gate cost for \hat{H}_I is 2 to 4 times that of \hat{H}_{KS} for the same number of qubits. Since \hat{H}_I should require $\gtrsim 2^d$ fewer qubits, for the interesting cases of $d = 2, 3$ we anticipate the same or fewer total gates to be required.

For \mathbb{Z}_2 gauge theory, \hat{H}_I can be mapped to Pauli matrices. Choosing the computational basis to be the group element basis, $\hat{U} = \hat{\sigma}^z$ and $\hat{L}^2 = \mathbb{1} - \hat{\sigma}^x$. Thus \mathcal{U}_\times is the CNOT gate. \mathcal{U}_{-1} is $\mathbb{1}$, and \mathcal{U}_F is the Hadamard gate. With these primitive gates, the circuit implementation for the $\mathcal{U}_{\text{V}_{\text{rect}}}$ and $\mathcal{U}_{K_{2L}}$ are found in Fig. 4a and Fig. 4b respectively.

One should ask what existing quantum errors are and what are required to benefit despite the additional circuit depth. As a test case, we implement the most expensive

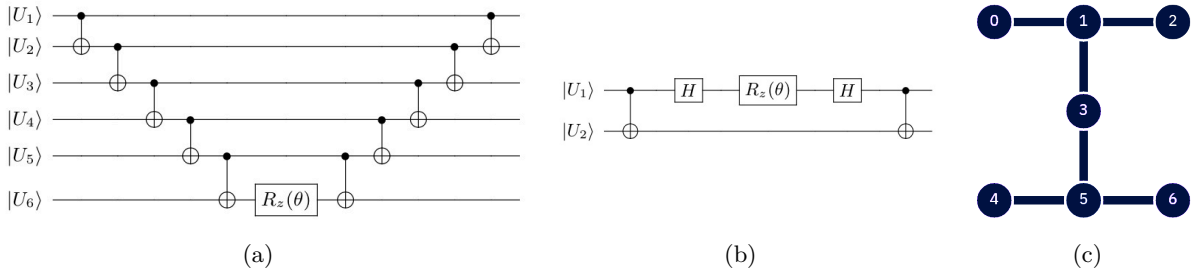


FIG. 4: (a) $\mathcal{U}_{V_{\text{rect}}}$ for \mathbb{Z}_2 gauge theory. (b) \mathcal{U}_{K_2L} for the \mathbb{Z}_2 gauge theory. (c) Connectivity map for `ibm_perth`.

\mathbb{Z}_2 gate, $\mathcal{U}_{V_{\text{rect}}}$, on the 7-qubit `ibm_perth` device (Fig. 4c) and study its fidelity. The connectivity of `ibm_perth` prevents implementing $\mathcal{U}_{V_{\text{rect}}}$ exactly as shown in Fig. 4a and a transpiled version of the circuit with 12 CNOTs and 20 additional one-qubit gates is used.

We consider the quantum fidelity metric $\mathcal{F}_q = \frac{1}{N} \sum_n \sqrt{|\langle \Psi_n | \mathcal{U}_{V_{\text{rect}}}^\dagger \mathcal{U}_{V_{\text{rect}}} | \Psi_n \rangle|^2}$ where the summands are defined as $\mathcal{F}_q^{[n]}$. For a noiseless simulation, each $\mathcal{F}_q^{[n]} = 1$ because the state preparation and $\mathcal{U}_{V_{\text{rect}}}$ are exactly cancelled by their complex conjugations, and thus the entire circuit is simply $\mathbb{1}$. Alas, accurately determining \mathcal{F}_q is prohibitively expensive since it requires summing over all possible $|\Psi_n\rangle$ – including entangled ones which introduce additional CNOT errors [79]. Therefore we consider a restricted set of unentangled initial states $|\Psi_n\rangle = \prod_m^n H_m^\otimes |000000\rangle$ where n indicates the number of qubits to which a Hadamard gate is applied. The strongly coupled vacuum state of \mathbb{Z}_2 corresponds to $|\Psi_6\rangle$. Taking the reported CNOT error rate of 2% [75–77] and assuming the CNOT errors are incoherent and state-independent, for $\mathcal{U}_{V_{\text{rect}}}$ one bounds the fidelity $\mathcal{F}_q \lesssim (0.98)^{12} = 0.78$. Evolving a two-plaquette lattice by \hat{H}_I for a single trotter step, \mathcal{U}_δ , requires at least 28 CNOTs and thus an upper bound of $\mathcal{F}_q^\delta \lesssim (0.98)^{28} = 0.56$.

In fact, the CNOT errors are expected to be dominated by coherent noise. To mitigate this, we implemented Pauli twirling [80–84] which allows us to convert coherent errors from various noise channels into random errors in Pauli channels and has found success in low-dimensional lattice field theories [85]. To do this, we modified the circuit by wrapping each CNOT with a set of Pauli gates $\{\mathbb{1}, X, Y, Z\}$ randomly sampled from sets which satisfy

$$\left(\prod_i (\sigma_i^{b_i})^\otimes \right) \text{CNOT} \otimes \mathbb{1}_4 \left(\prod_i (\sigma_i^{a_i})^\otimes \right) = \text{CNOT} \otimes \mathbb{1}_4, \quad (12)$$

where the i -th qubit (including spectators) was rotated by $\sigma_i^{a_i}$ before the CNOT and by $\sigma_i^{b_i}$ after. For our 24-CNOT $\mathcal{U}_{V_{\text{rect}}}^\dagger \mathcal{U}_{V_{\text{rect}}}$ circuit there are 16 ways to twirl the target and control qubits, and 4 ways to twirl the 4 spectators, so $(16 \times 4^4)^{24} \sim 10^{87}$ possible circuits. Prior work found that sampling $\mathcal{O}(10)$ circuits was sufficient [80], thus we

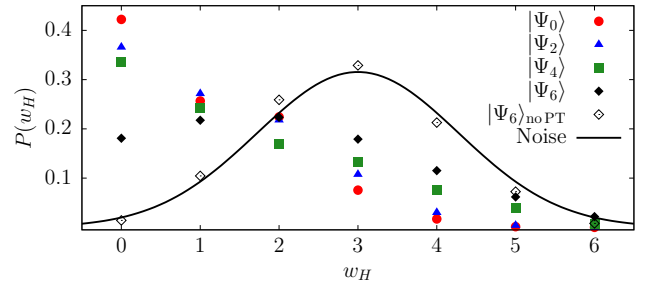


FIG. 5: Observed probability of measuring Hamming weights for selected $|\Psi_n\rangle$ compared to the noise-dominated results. Note that $\sqrt{P(w_H=0)} = \mathcal{F}_q^{[n]}$.

ran 15 unique circuits each with $N_{\text{shots}} = 2^{13}$. We also computed $\mathcal{F}_q^{[6]}$ without Pauli twirling to gauge its effect.

In the zero-noise limit, the expected measurement for all $|\Psi_n\rangle$ should be all shots in the $|000000\rangle$ state. Thus, we can infer information about the noise by comparing the probability of measuring this state to all others. One way to group the data is by the number of 1-bits observed – the Hamming weight w_H . We present results for these probabilities $P(w_H)$ for selected $|\Psi_n\rangle$ in Fig. 5. In the noise-dominated limit, one expects all states are equally populated with $P(w_H) \propto \binom{6}{w_H}$. For the $n=6$ state without Pauli twirling ($|\Psi_6\rangle_{\text{no,PT}}$), we observed that $P(w_H)$ is indistinguishable from the noise-dominated limit while all the Pauli-twirled results are skewed toward the noiseless result, with states of lower n (and consequently less average entanglement) being closer to the desired value.

Our measured $\mathcal{F}_q^{[n]} = \sqrt{P(w_H=0)}$ from `ibm_perth` are presented in Table II. Comparing the results for $|\Psi_6\rangle$ with and without Pauli twirling we observe a fourfold improvement in fidelity – clearly demonstrating the advantage gained from this error mitigation. Together these results yield $\mathcal{F}_q = 0.550$ for $\mathcal{U}_{V_{\text{rect}}}$.

Using this refined upper bound on \mathcal{F}_q , we can estimate $\mathcal{F}_q^\delta \lesssim 0.25$ based on it containing $\frac{28}{12}$ more CNOTs. This low \mathcal{F}_q^δ suggests that while current devices are inadequate for dynamics, a two-plaquette \mathbb{Z}_2 lattice appears possible in the next two years given the expected hardware improvements [44–46], allowing for direct comparisons

$ \Psi_n\rangle$	$ \Psi_0\rangle$	$ \Psi_1\rangle$	$ \Psi_2\rangle$	$ \Psi_3\rangle$	$ \Psi_4\rangle$	$ \Psi_5\rangle$	$ \Psi_6\rangle$	$ \Psi_6\rangle_{\text{no PT}}$
$\mathcal{F}_q^{[n]}$	0.650	0.575	0.605	0.599	0.579	0.442	0.425	0.1194

TABLE II: Measured state-dependent quantum fidelities with and without Pauli twirling.

between Hamiltonians. Alternatively, classical simulators could explore larger lattices up to 7^2 [86].

In this *letter*, we designed the quantum circuits for simulating the Symanzik-improved Hamiltonian. In comparison to \hat{H}_{KS} , \hat{H}_I should allow quantum simulations with $\gtrsim 2^d$ fewer qubits. With this reduction, we expect the gate count is comparable or less than that for \hat{H}_{KS} for theories with $d \geq 2$ despite increases of gate costs per link. For near-term numerical demonstrations, we constructed the circuits for \hat{H}_I of the \mathbb{Z}_2 gauge group and found that for `ibm_perth` the fidelity of the 12 CNOT improved potential term is $\lesssim 0.550$. Our results suggest that alongside hardware improvements, improved Hamiltonians can accelerate quantum simulations by years, with optimistic prospects for $2 + 1d$ \mathbb{Z}_2 simulations in the near future.

We would like to thank Erik Gustafson for helpful comments. This work is supported by the Department of Energy through the Fermilab QuantISED program in the area of “Intersections of QIS and Theoretical Particle Physics”. Fermilab is operated by Fermi Research Alliance, LLC under contract number DE-AC02-07CH11359 with the United States Department of Energy. We acknowledge use of the IBM Q for this work. The views expressed are those of the authors and do not reflect the official policy or position of IBM or the IBM Q team.

-
- [1] R. P. Feynman, Simulating physics with computers, *Int. J. Theor. Phys.* **21**, 467 (1982).
- [2] S. P. Jordan, H. Krovi, K. S. Lee, and J. Preskill, BQP-completeness of Scattering in Scalar Quantum Field Theory, *Quantum* **2**, 44 (2018), [arXiv:1703.00454 \[quant-ph\]](#).
- [3] M. C. Bañuls *et al.*, Simulating Lattice Gauge Theories within Quantum Technologies, *Eur. Phys. J. D* **74**, 165 (2020), [arXiv:1911.00003 \[quant-ph\]](#).
- [4] T. D. Cohen, H. Lamm, S. Lawrence, and Y. Yamauchi (NuQS), Quantum algorithms for transport coefficients in gauge theories, *Phys. Rev. D* **104**, 094514 (2021), [arXiv:2104.02024 \[hep-lat\]](#).
- [5] H. Lamm, S. Lawrence, and Y. Yamauchi (NuQS), Parton physics on a quantum computer, *Phys. Rev. Res.* **2**, 013272 (2020), [arXiv:1908.10439 \[hep-lat\]](#).
- [6] M. Kreshchuk, W. M. Kirby, G. Goldstein, H. Beauchemin, and P. J. Love, Quantum Simulation of Quantum Field Theory in the Light-Front Formulation (2020), [arXiv:2002.04016 \[quant-ph\]](#).
- [7] M. Echevarria, I. Egusquiza, E. Rico, and G. Schnell, Quantum Simulation of Light-Front Parton Correlators (2020), [arXiv:2011.01275 \[quant-ph\]](#).
- [8] B. Chakraborty, M. Honda, T. Izubuchi, Y. Kikuchi, and A. Tomiya, Digital Quantum Simulation of the Schwinger Model with Topological Term via Adiabatic State Preparation (2020), [arXiv:2001.00485 \[hep-lat\]](#).
- [9] M. Honda, E. Itou, Y. Kikuchi, L. Nagano, and T. Okuda, Digital quantum simulation for screening and confinement in gauge theory with a topological term (2021), [arXiv:2105.03276 \[hep-lat\]](#).
- [10] A. Alexandru, P. F. Bedaque, S. Harmalkar, H. Lamm, S. Lawrence, and N. C. Warrington (NuQS), Gluon field digitization for quantum computers, *Phys. Rev. D* **100**, 114501 (2019), [arXiv:1906.11213 \[hep-lat\]](#).
- [11] I. Raychowdhury and J. R. Stryker, Solving Gauss’s Law on Digital Quantum Computers with Loop-String-Hadron Digitization (2018), [arXiv:1812.07554 \[hep-lat\]](#).
- [12] I. Raychowdhury and J. R. Stryker, Loop, String, and Hadron Dynamics in SU(2) Hamiltonian Lattice Gauge Theories, *Phys. Rev. D* **101**, 114502 (2020), [arXiv:1912.06133 \[hep-lat\]](#).
- [13] Z. Davoudi, I. Raychowdhury, and A. Shaw, Search for Efficient Formulations for Hamiltonian Simulation of non-Abelian Lattice Gauge Theories (2020), [arXiv:2009.11802 \[hep-lat\]](#).
- [14] A. Ciavarella, N. Klco, and M. J. Savage, A Trailhead for Quantum Simulation of SU(3) Yang-Mills Lattice Gauge Theory in the Local Multiplet Basis (2021), [arXiv:2101.10227 \[quant-ph\]](#).
- [15] A. Kan and Y. Nam, Lattice Quantum Chromodynamics and Electrodynamics on a Universal Quantum Computer (2021), [arXiv:2107.12769 \[quant-ph\]](#).
- [16] A. Alexandru, P. F. Bedaque, R. Brett, and H. Lamm, The spectrum of qubitized QCD: glueballs in a $S(1080)$ gauge theory (2021), [arXiv:2112.08482 \[hep-lat\]](#).
- [17] E. Zohar, J. I. Cirac, and B. Reznik, Cold-Atom Quantum Simulator for SU(2) Yang-Mills Lattice Gauge Theory, *Phys. Rev. Lett.* **110**, 125304 (2013), [arXiv:1211.2241 \[quant-ph\]](#).
- [18] E. Zohar, J. I. Cirac, and B. Reznik, Quantum simulations of gauge theories with ultracold atoms: local gauge invariance from angular momentum conservation, *Phys. Rev. A* **88**, 023617 (2013), [arXiv:1303.5040 \[quant-ph\]](#).
- [19] E. Zohar and M. Burrello, Formulation of lattice gauge theories for quantum simulations, *Phys. Rev. D* **91**, 054506 (2015), [arXiv:1409.3085 \[quant-ph\]](#).
- [20] E. Zohar, A. Farace, B. Reznik, and J. I. Cirac, Digital lattice gauge theories, *Phys. Rev. A* **95**, 023604 (2017), [arXiv:1607.08121 \[quant-ph\]](#).
- [21] J. Bender, E. Zohar, A. Farace, and J. I. Cirac, Digital quantum simulation of lattice gauge theories in three spatial dimensions, *New J. Phys.* **20**, 093001 (2018), [arXiv:1804.02082 \[quant-ph\]](#).
- [22] J. F. Haase, L. Dellantonio, A. Celi, D. Paulson, A. Kan, K. Jansen, and C. A. Muschik, A resource efficient approach for quantum and classical simulations of gauge theories in particle physics, *Quantum* **5**, 393 (2021), [arXiv:2006.14160 \[quant-ph\]](#).
- [23] C. W. Bauer and D. M. Grabowska, Efficient Representation for Simulating U(1) Gauge Theories on Digital Quantum Computers at All Values of the Coupling (2021), [arXiv:2111.08015 \[hep-ph\]](#).
- [24] Y. Ji, H. Lamm, and S. Zhu (NuQS), Gluon Field Digitization via Group Space Decimation for Quantum Computers, *Phys. Rev. D* **102**, 114513 (2020), [arXiv:2005.14221 \[hep-lat\]](#).

- [25] A. Bazavov, S. Catterall, R. G. Jha, and J. Unmuth-Yockey, Tensor renormalization group study of the non-abelian higgs model in two dimensions, *Phys. Rev. D* **99**, 114507 (2019).
- [26] A. Bazavov, Y. Meurice, S.-W. Tsai, J. Unmuth-Yockey, and J. Zhang, Gauge-invariant implementation of the Abelian Higgs model on optical lattices, *Phys. Rev.* **D92**, 076003 (2015), [arXiv:1503.08354 \[hep-lat\]](#).
- [27] J. Zhang, J. Unmuth-Yockey, J. Zeiher, A. Bazavov, S. W. Tsai, and Y. Meurice, Quantum simulation of the universal features of the Polyakov loop, *Phys. Rev. Lett.* **121**, 223201 (2018), [arXiv:1803.11166 \[hep-lat\]](#).
- [28] J. Unmuth-Yockey, J. Zhang, A. Bazavov, Y. Meurice, and S.-W. Tsai, Universal features of the Abelian Polyakov loop in 1+1 dimensions, *Phys. Rev.* **D98**, 094511 (2018), [arXiv:1807.09186 \[hep-lat\]](#).
- [29] J. F. Unmuth-Yockey, Gauge-invariant rotor Hamiltonian from dual variables of 3D $U(1)$ gauge theory, *Phys. Rev. D* **99**, 074502 (2019), [arXiv:1811.05884 \[hep-lat\]](#).
- [30] U.-J. Wiese, Towards Quantum Simulating QCD, *Proceedings, 24th International Conference on Ultra-Relativistic Nucleus-Nucleus Collisions (Quark Matter 2014): Darmstadt, Germany, May 19-24, 2014*, *Nucl. Phys.* **A931**, 246 (2014), [arXiv:1409.7414 \[hep-th\]](#).
- [31] D. Luo, J. Shen, M. Highman, B. K. Clark, B. DeMarco, A. X. El-Khadra, and B. Gadway, A Framework for Simulating Gauge Theories with Dipolar Spin Systems (2019), [arXiv:1912.11488 \[quant-ph\]](#).
- [32] R. C. Brower, D. Berenstein, and H. Kawai, Lattice Gauge Theory for a Quantum Computer, *PoS LATTICE2019*, 112 (2019), [arXiv:2002.10028 \[hep-lat\]](#).
- [33] S. V. Mathis, G. Mazzola, and I. Tavernelli, Toward scalable simulations of Lattice Gauge Theories on quantum computers, *Phys. Rev. D* **102**, 094501 (2020), [arXiv:2005.10271 \[quant-ph\]](#).
- [34] H. Liu and S. Chandrasekharan, Qubit Regularization and Qubit Embedding Algebras (2021), [arXiv:2112.02090 \[hep-lat\]](#).
- [35] E. Gustafson, Prospects for Simulating a Qudit Based Model of (1+1)d Scalar QED, *Phys. Rev. D* **103**, 114505 (2021), [arXiv:2104.10136 \[quant-ph\]](#).
- [36] E. Gustafson, Noise Improvements in Quantum Simulations of sQED using Qutrits (2022), [arXiv:2201.04546 \[quant-ph\]](#).
- [37] J. Kogut and L. Susskind, Hamiltonian formulation of Wilson's lattice gauge theories, *Phys. Rev. D* **11**, 395 (1975).
- [38] E. Zohar, J. I. Cirac, and B. Reznik, Quantum Simulations of Lattice Gauge Theories using Ultracold Atoms in Optical Lattices, *Rept. Prog. Phys.* **79**, 014401 (2016), [arXiv:1503.02312 \[quant-ph\]](#).
- [39] Y. Tong, V. V. Albert, J. R. McClean, J. Preskill, and Y. Su, Provably accurate simulation of gauge theories and bosonic systems (2021), [arXiv:2110.06942 \[quant-ph\]](#).
- [40] A. F. Shaw, P. Lougovski, J. R. Stryker, and N. Wiebe, Quantum Algorithms for Simulating the Lattice Schwinger Model, *Quantum* **4**, 306 (2020), [arXiv:2002.11146 \[quant-ph\]](#).
- [41] H. B. Meyer, Transport Properties of the Quark-Gluon Plasma: A Lattice QCD Perspective, *Eur. Phys. J. A* **47**, 86 (2011), [arXiv:1104.3708 \[hep-lat\]](#).
- [42] B. Şahinoğlu and R. D. Somma, Hamiltonian simulation in the low energy subspace (2020), [arXiv:2006.02660 \[quant-ph\]](#).
- [43] T. Hatomura, State-dependent error bound for digital quantum simulation of driven systems (2022), [arXiv:2201.04835 \[quant-ph\]](#).
- [44] [Scaling IonQ's quantum computers: The roadmap \(2020\)](#).
- [45] [IBM's roadmap for building an open quantum software ecosystem \(2021\)](#).
- [46] H. Neven, [Day 1 opening keynote by Hartmut Neven \(quantum summer symposium 2020\) \(2020\)](#).
- [47] E. Campbell, Random compiler for fast Hamiltonian simulation, *Phys. Rev. Lett.* **123**, 070503 (2019).
- [48] C. Cirstoiu, Z. Holmes, J. Iosue, L. Cincio, P. J. Coles, and A. Sornborger, Variational fast forwarding for quantum simulation beyond the coherence time, *npj Quantum Information* **6**, 1 (2020).
- [49] J. Gibbs, K. Gili, Z. Holmes, B. Commeau, A. Arrasmith, L. Cincio, P. J. Coles, and A. Sornborger, Long-time simulations with high fidelity on quantum hardware (2021), [arXiv:2102.04313 \[quant-ph\]](#).
- [50] Y.-X. Yao, N. Gomes, F. Zhang, T. Iadecola, C.-Z. Wang, K.-M. Ho, and P. P. Orth, Adaptive variational quantum dynamics simulations, [arXiv preprint arXiv:2011.00622 \(2020\)](#).
- [51] D. W. Berry, A. M. Childs, R. Cleve, R. Kothari, and R. D. Somma, Simulating Hamiltonian dynamics with a truncated Taylor series, *Phys. Rev. Lett.* **114**, 090502 (2015).
- [52] G. H. Low and I. L. Chuang, Hamiltonian Simulation by Qubitization, *Quantum* **3**, 163 (2019).
- [53] H. Lamm and S. Lawrence, Simulation of Nonequilibrium Dynamics on a Quantum Computer, *Phys. Rev. Lett.* **121**, 170501 (2018), [arXiv:1806.06649 \[quant-ph\]](#).
- [54] S. Harmalkar, H. Lamm, and S. Lawrence (NuQS), Quantum Simulation of Field Theories Without State Preparation (2020), [arXiv:2001.11490 \[hep-lat\]](#).
- [55] E. J. Gustafson and H. Lamm, Toward quantum simulations of \mathbb{Z}_2 gauge theory without state preparation, *Phys. Rev. D* **103**, 054507 (2021), [arXiv:2011.11677 \[hep-lat\]](#).
- [56] Y. Yang, B.-N. Lu, and Y. Li, Accelerated Quantum Monte Carlo with Mitigated Error on Noisy Quantum Computer, *PRX Quantum* **2**, 040361 (2021), [arXiv:2106.09880 \[quant-ph\]](#).
- [57] K. Osterwalder and R. Schrader, Axioms for Euclidean Green's Functions, *Commun. Math. Phys.* **31**, 83 (1973).
- [58] K. Osterwalder and R. Schrader, Axioms for Euclidean Green's Functions. 2., *Commun. Math. Phys.* **42**, 281 (1975).
- [59] M. Carena, H. Lamm, Y.-Y. Li, and W. Liu, Lattice Renormalization of Quantum Simulations (2021), [arXiv:2107.01166 \[hep-lat\]](#).
- [60] A. Rajput, A. Roggero, and N. Wiebe, Quantum error correction with gauge symmetries (2021), [arXiv:2112.05186 \[quant-ph\]](#).
- [61] N. Klco and M. J. Savage, Hierarchical qubit maps and hierarchically implemented quantum error correction, *Physical Review A* **104**, 10.1103/physreva.104.062425 (2021).
- [62] K. Symanzik, Continuum Limit and Improved Action in Lattice Theories. 1. Principles and ϕ^4 Theory, *Nucl. Phys. B* **226**, 187 (1983).
- [63] M. Luscher and P. Weisz, On-Shell Improved Lattice Gauge Theories, *Commun. Math. Phys.* **97**, 59 (1985), [Erratum: *Commun. Math. Phys.* 98,433(1985)].
- [64] M. Luscher and P. Weisz, Computation of the Action for On-Shell Improved Lattice Gauge Theories at Weak Coupling, *Phys. Lett. B* **158**, 250 (1985).

- [65] X.-Q. Luo, S.-H. Guo, H. Kroger, and D. Schutte, Improved lattice gauge field Hamiltonian, *Phys. Rev. D* **59**, 034503 (1999), [arXiv:hep-lat/9804029](#).
- [66] J. Carlsson and B. H. McKellar, Direct improvement of Hamiltonian lattice gauge theory, *Phys. Rev. D* **64**, 094503 (2001), [arXiv:hep-lat/0105018](#).
- [67] G. P. Lepage, Redesigning lattice qcd, *Lecture Notes in Physics*, 1–48.
- [68] M. G. Alford, W. Dimm, G. P. Lepage, G. Hockney, and P. B. Mackenzie, Lattice QCD on small computers, *Phys. Lett. B* **361**, 87 (1995), [arXiv:hep-lat/9507010](#).
- [69] J. Carlsson, *Improvement and analytic techniques in Hamiltonian lattice gauge theory*, Other thesis (2003), [arXiv:hep-lat/0309138](#).
- [70] G. P. Lepage and P. B. Mackenzie, Viability of lattice perturbation theory, *Physical Review D* **48**, 2250–2264 (1993).
- [71] M. Alford, W. Dimm, G. Lepage, G. Hockney, and P. Mackenzie, Lattice qcd on small computers, *Physics Letters B* **361**, 87–94 (1995).
- [72] D. Spitz and J. Berges, Schwinger pair production and string breaking in non-Abelian gauge theory from real-time lattice improved Hamiltonians, *Phys. Rev. D* **99**, 036020 (2019), [arXiv:1812.05835 \[hep-ph\]](#).
- [73] H. Lamm, S. Lawrence, and Y. Yamauchi (NuQS), General Methods for Digital Quantum Simulation of Gauge Theories, *Phys. Rev. D* **100**, 034518 (2019), [arXiv:1903.08807 \[hep-lat\]](#).
- [74] A. F. Izmaylov, On construction of projection operators, *The Journal of Physical Chemistry A* **123**, 3429–3433 (2019).
- [75] K. Wei, E. Magesan, I. Lauer, S. Srinivasan, D. Bogorin, S. Carnevale, G. Keefe, Y. Kim, D. Klaus, W. Landers, *et al.*, Quantum crosstalk cancellation for fast entangling gates and improved multi-qubit performance (2021), [arXiv:2106.00675 \[quant-ph\]](#).
- [76] L. Lao, A. Korotkov, Z. Jiang, W. Mruczkiewicz, T. E. O’Brien, and D. E. Browne, Software mitigation of coherent two-qubit gate errors (2021), [arXiv:2111.04669 \[quant-ph\]](#).
- [77] L. Howe, M. Castellanos-Beltran, A. J. Sirois, D. Olaya, J. Biesecker, P. D. Dresselhaus, S. P. Benz, and P. F. Hopkins, Digital control of a superconducting qubit using a Josephson pulse generator at 3 K (2021), [arXiv:2111.12778 \[quant-ph\]](#).
- [78] M. S. Alam, S. Hadfield, H. Lamm, and A. C. Y. Li, Quantum Simulation of Dihedral Gauge Theories (2021), [arXiv:2108.13305 \[quant-ph\]](#).
- [79] I. L. Chuang and M. A. Nielsen, Prescription for experimental determination of the dynamics of a quantum black box, *J. Mod. Opt.* **44**, 2455 (1997), [arXiv:quant-ph/9610001](#).
- [80] A. Erhard, J. J. Wallman, L. Postler, M. Meth, R. Stricker, E. A. Martinez, P. Schindler, T. Monz, J. Emerson, and R. Blatt, Characterizing large-scale quantum computers via cycle benchmarking, *Nature Communications* **10**, 10.1038/s41467-019-13068-7 (2019).
- [81] Y. Li and S. C. Benjamin, Efficient variational quantum simulator incorporating active error minimization, *Physical Review X* **7**, 021050 (2017).
- [82] S. Endo, S. C. Benjamin, and Y. Li, Practical quantum error mitigation for near-future applications, *Physical Review X* **8**, 10.1103/physrevx.8.031027 (2018).
- [83] M. R. Geller and Z. Zhou, Efficient error models for fault-tolerant architectures and the pauli twirling approximation, *Physical Review A* **88**, 10.1103/physreva.88.012314 (2013).
- [84] J. J. Wallman and J. Emerson, Noise tailoring for scalable quantum computation via randomized compiling, *Physical Review A* **94**, 10.1103/physreva.94.052325 (2016).
- [85] K. Yeter-Aydeniz, Z. Parks, A. Nair, E. Gustafson, A. F. Kemper, R. C. Pooser, Y. Meurice, and P. Dreher, Measuring NISQ Gate-Based Qubit Stability Using a 1+1 Field Theory and Cycle Benchmarking (2022), [arXiv:2201.02899 \[quant-ph\]](#).
- [86] E. Gustafson *et al.*, Large scale multi-node simulations of \mathbb{Z}_2 gauge theory quantum circuits using Google Cloud Platform, in *IEEE/ACM Second International Workshop on Quantum Computing Software* (2021) [arXiv:2110.07482 \[quant-ph\]](#).